Biogeochemistry **26**: 145–161, 1994.

Biogeochemical cycling of sulfur and iron in sediments of a south-east Asian mangrove, Phuket Island, Thailand

MARIANNE HOLMER[1,*], ERIK KRISTENSEN[1], GARY BANTA[1], KIM HANSEN[1], MIKAEL HJORTH JENSEN[1] & NIPUVAN BUSSAWARIT[2]

[1] *Institute of Biology, Odense University, Campusvej 55, DK-5230 Odense M, Denmark;*
[2] *Phuket Marine Biological Center, P.O. Box 60, Phuket, 83000 Thailand; *Author of correspondence. Present address: Department of Life Sciences and Chemistry, 17.2, Roskilde University, P.O. Box 260, DK-4000 Roskilde, Denmark*

Received 19 November 1993; accepted in revised form 23 May 1994

Key words: mangrove sediments, sulfate reduction, sulfur and iron dynamics

Abstract. Benthic sulfate reduction and sediment pools of sulfur and iron were examined during January 1992 at 3 stations in the Ao Nam Bor mangrove, Phuket, Thailand. Patterns of sulfate reduction rates (0–53 cm) reflected differences in physical and biological conditions at the 3 stations, and highest rates were found at the vegetated site within the mangrove (*Rhizophora apiculata*) forest. Due to extended oxidation of mangrove sediments, a large portion of the added ^{35}S-label was recovered in the chromium reducible pools (FeS_2 and S^0) (41–91% of the reduced sulfur). Pyrite was the most important inorganic sulfur component, attaining pool sizes 50–100 times higher than acid volatile pools (FeS). HCl-extractable (0.5 M HCl) iron pools, including $Fe(II)_{HCl}$ and $Fe(III)_{HCl}$, were generally low and $Fe(III)_{HCl}$ was only present in the upper surface layers (0–5 cm). Maximum concentrations of dissolved Fe^{2+} (35–285 μM) occurred just about the depth where dissolved ΣH_2S accumulated. Furthermore Fe^{2+} and ΣH_2S coexisted only where concentrations of both were low. There was an accumulation of organic sulfur in the deep sediment at 2 stations in the inner part of the mangrove. The reoxidation of reduced sulfides was rapid, and storage of sulfur was minor in the upper sediment layers, where factors like bioturbation, the presence of roots, or tidal mixing enhance oxidation processes.

Introduction

The biogeochemical role of sulfur in marine sediments, i.e., sulfate reduction, pyrite and organic sulfur formation and metal cycling, is an area of intense research (Jørgensen 1982; Howarth 1984; Skyring 1987; Giblin 1988; Canfield 1989; Thode-Andersen & Jørgensen 1989; Ferdelman et al. 1991). Sulfate reduction and burial of sulfur in the form of pyrite and organic sulfur have previously been observed in mangrove sediments (Casagrande et al. 1977; Altschuler et al. 1983; Kristensen et al. 1991, 1992). Little is known, however, about the actual mechanisms and control of specific processes involved in mangrove sulfur cycling. Although sulfur compounds generally are important for energy transfer and element cycling in tidal sediments (Howarth 1984; Giblin 1988; Oenema 1990), pyrite formation and oxidation

in mangrove sediments may also have significant impacts on the benthic community due to a variety of secondary effects, e.g., associated pH changes (Hart 1959; Gardner 1973; Howarth et al. 1983; Giblin & Howarth 1984; Mongia & Ganeshamurthy 1989; Luther et al. 1991).

The accumulation of sulfur in marine sediments is primarily controlled by the rate of sulfate reduction and the oxidation state of the sediment. In subtidal environments the input of organic matter and bioturbation generally determine the rates of sulfate reduction and sulfide oxidation (Howarth 1984; Skyring 1987; King 1988; Fossing et al. 1992). In tidal environments, however, additional factors must be considered. Tidal currents and wave action may affect the oxidation status of sediments directly by increased advective transport of pore water and particles (Giblin & Howarth 1984; Oenema 1990; Huettel 1992). During low tide the sediment surface desiccates and oxygen may penetrate deeper into the sediment via burrows and cracks in the surface (Andersen & Kristensen 1988; Luther et al. 1991; Kristensen et al. 1992). The presence of rooted vegetation, such as those found in salt marshes and mangroves, strongly affects the biogeochemical cycling of elements like sulfur and iron by vertical translocation of organic matter and oxygen (Carlson et al. 1983; Higashi & Shinagawa 1985; Luther et al. 1985; Thibodeau & Nickerson 1986; Giblin 1988; King 1988; McKee et al. 1988; Hines et al. 1989; Mongia & Ganeshamurthy 1989; Ferdelman et al. 1991).

The cycling of sulfur in sediment is closely coupled to the reactive iron pools. Reactive iron oxides present in sediments may efficiently oxidize reduced sulfides. In fact, the partitioning between oxidized and reduced iron may determine the rate of sulfide oxidation (Canfield 1989; Canfield et al. 1992; Moses & Herman 1991; Fossing et al. 1992). In deep and reduced sediment layers, the precipitation of iron sulfides in various forms is an important process in terms of sulfur burial.

This study concerns the biogeochemical cycling of sulfur and iron in sediments of the Ao Nam Bor mangrove forest, Thailand. Three different sediment types were examined in the forest: a high-intertidal non-vegetated sediment at the landward fringe, a vegetated and rooted sediment in the mangrove proper, and a non-vegetated sediment of the low-intertidal flat outside the mangrove forest. Measurements of sulfate reduction were related to solid phase and pore water pools of various sulfur and iron species. Parallel studies of benthic metabolism and nitrogen cycling are to be found elsewhere (Kristensen et al. 1994; Jensen et al. in prep.).

Materials and methods

Study site. Three stations were examined during January 1992 in the Ao Nam Bor mangrove forest, Phuket Island, Thailand (Kristensen et al. 1991). The high-intertidal station close to the landward fringe, Sta. 1, was situated on a non-vegetated bank adjacent to a small (ca. 1 m wide) creek. This station,

which was only flooded during spring tides, was heavily impacted by crab burrows (1046 ± 508 m^{-2}; length 10–20 cm) resulting in a sediment with a thick (5–10 cm) oxidized surface layer. The mid-intertidal mangrove sediment (Sta. 2) was situated within the mangrove forest ca. 30 m from a 4 m wide creek and was influenced by both living and dead roots of *Rhizophora apiculata*. The intensity of bioturbation was moderate (41 ± 6 crab burrows m^{-2}, 500 ± 62 sipunculids m^{-2}). The low-intertidal station (Sta. 3) was situated on a non-vegetated sand- and mudflat ca. 100 m outside the forest and was strongly influenced by tidal currents and wave action. The bioturbating macrofauna (8 ± 1 crab burrows m^{-2}, 1400 ± 600 small polychaetes m^{-2}, 5 mudskippers m^{-2}) generally occupied more or less permanent burrows. A detailed description of the study site is given by Kristensen et al. (1991).

Pore water sampling and analysis. Three long cores (i.d. = 5.0 cm) for determination of pore water sulfate and chloride concentrations, alkalinity and pH were collected at each station by hand at low tide (Sta. 1, 36 cm; Sta. 2, 36 cm; and Sta. 3, 48 cm deep). The sediment was sectioned into 1-cm segments in the upper 4 cm, and 2-cm segments below. Pore water was extracted by centrifugation (1500 rpm, 7 min). Samples for sulfate and chloride were preserved with HCl (pH < 2), and stored at 5 °C until analysis. The samples were analyzed by ion chromatography and UV-detection (inverse photometry) with potassium-phthalate as the eluent. Pore water for pH and alkalinity analysis was kept at 5 °C and analysed within 12 hours. Alkalinity was determined by titration with 0.01 M HCl. Two cores from each station were sectioned in a glove-bag under N_2 atmosphere and centrifuged (1500 rpm, 4 min) in closed tubes, enclosing a N_2 atmosphere, to extract pore water from analysis of dissolved sulfides (ΣH_2S) and ferrous iron, Fe^{2+}. Samples for ΣH_2S were fixed in 0.1 M ZnAc and analyzed by the method of Cline (1969). Iron samples were preserved (1:2) in 0.1% Ferrozine (in 50 mM HEPES buffer, pH 7) and analyzed colorimetrically according to Stookey (1970) as modified by Sørensen (1982).

Sulfate reduction rates and inorganic sulfur pools. Two cores (i.d. = 2.6 cm, l = 16 cm) and one core (i.d. = 5 cm, l = 35–53 cm) were collected from each station for the sulfate reduction assay. The long core was subsequently subcored into smaller cores (i.d. = 2.6 cm, l = 16 cm) with silicone-filled injection ports. Sulfate reduction was measured by the core injection technique (Jørgensen 1978). A volume of 2 µl of carrier-free ^{35}S–SO_4^{2-} (70 kBq) was injected at 1-cm intervals and the cores were incubated with an exposed surface in darkness for 12 h at the *in situ* temperature (28 °C). Each subcore was sectioned in 1 to 2 cm segments and fixed in 1 M ZnAc. The samples were stored frozen until they were analysed within 1–3 months.

A 2-step distillation procedure (acid volatile sulfides, AVS, and chromium reducible sulfur, CRS) was used for one core from each station, and a 1-step procedure (total reducible inorganic sulfur, TRIS) for the other two cores

(Fossing & Jørgensen 1989). The sediment was washed 3 times to remove $^{35}S–SO_4^{2-}$, and about 2 g of each sediment pellet was transferred to a reaction flask with 10 ml 50% ethanol. In the 2-step procedure AVS was liberated as H_2S after degassing and acidification (8 ml 12 M HCl) at room temperature with continuous stirring for 30 min using N_2 as a carrier gas. The sulfide was trapped as ZnS in 10 ml 0.25 M ZnAc. Afterwards, CRS was determined by adding 16 ml 1 M Cr^{2+} in 0.5 M HCl followed by boiling for 30 min after inserting a new ZnAc trap. During the 1-step (TRIS) procedure both reagents were added at the start and the distillation was run for 40 min. Radioactivity of ^{35}S in the supernatant and the traps were determined on subsamples using a Packard 2200 CA TRI-CARB Scintillation Analyzer.

Sulfide concentrations in the traps were analysed as described above for pore water sulfide concentrations to obtain the pools of inorganic reduced sulfur in the sediment.

Inorganic iron pools. Solid phase iron was determined by HCl-extraction using hydroxylamine to distinguish extracted $Fe(III)_{HCl}$ from $Fe(II)_{HCl}$ after procedures given by Lovley & Philips (1987) with slight modifications (Thamdrup, pers comm.; Fossing et al. 1992). Immediately after a core was sectioned, a 50–200 mg subsample of homogenized sediment was quickly transferred to serum bottles containing 5 ml 0.5 M HCl. Extractions were done for 1 h on a shaking table at 20 °C. Following centrifugation, 50 µl of the supernatant was transferred to 2 ml Ferrozine solution (0.02% Ferrozine in 50 mM HEPES buffer, pH 7) for spectrophotometric analysis of Fe^{2+} (Stookey 1970). Another 1-ml subsample of the supernatant was transferred to test tubes containing 0.2 ml 1.5 M hydroxylamine hydrochloride in 0.25 M HCl. After occasional shaking for 15 min, 50 µl was mixed with 2 ml Ferrozine solution and analyzed as mentioned above. This procedure gave the total extracted Fe content, i.e. $Fe(II)_{HCl}$ + $Fe(III)_{HCl}$; $Fe(III)_{HCl}$ was determined by difference.

Sediment characteristics. Total pools of particulate organic and inorganic carbon, nitrogen and sulfur were determined down to 30 cm depth on subsamples from the cores used for pore water extraction by the method described by Kristensen & Andersen (1987) using a Carlo Erba Elemental Analyzer EA 1100A.

Results

Sediment characteristics. The very slow and infrequent tidal currents at Sta. 1 allowed for the deposition of a thick slit layer. Organic content varied irregularly with depth: 1100–2200 µmol POC g dw^{-1} and 40–54 µmol PON g dw^{-1} (data not shown). The numerous burrows were responsible for a 5 to 10 cm thick, continuous brown oxidized upper zone. Deeper down, the oxidized zone was restricted to a ~5 mm radial layer around the burrows.

Sta. 2 was less affected by burrowing fauna. The sediment consisted of a 6–8 cm grey silt zone with small and scattered roots overlying a peat-like root zone down to at least 40 cm. Throughout the sediment scattered black spots were observed. Organic content increased with depth from 2100 µmol POC g dw^{-1}, 80 µmol PON g dw^{-1} (upper 5 cm) to 3100 µmol POC g dw^{-1} and 107 µmol PON g dw^{-1} at 20–30 cm depth.

At the tidal flat (Sta. 3), the sediment appeared more sandy and consisted of silty sand down to a depth of ca. 30 cm followed by a 5–10 cm zone of coarse coral sand. The upper 0–4 cm of the sediment was oxidized. Below, a grey reduced zone dominated down to the coral sand layer. The organic content increased with depth from 230 µmol POC g dw^{-1} and 8 µmol PON g dw^{-1} (0–4 cm) to 1400 µmol POC g dw^{-1} and 32 µmol PON g dw^{-1} in the deeper layers (4–30 cm).

Sulfate reduction. Sulfate reduction rates (SRR) at Sta. 1 and 3 were low in the surface layers (Fig. 1), while maximum rates were found at 4–10 cm depth (105 and 115 nmol cm^{-3} d^{-1} respectively). Below, SRR gradually declined to low rates. At Sta. 2, sulfate reduction was high in the uppermost cm (115 nmol cm^{-3} d^{-1}). A subsequent minimum was recorded at 2–3 cm depth followed by a maximum (170 nmol cm^{-3} d^{-1}) coinciding with the transition between the silt and root zone at 6–8 cm depth. A decrease in SRR occurred below 12 cm depth at this station.

The fraction of label recovered as ^{35}S-AVS (ΣH_2S + FeS) increased with depth at all 3 stations until a maximum was reached at 6–12 cm depth (Sta. 1 and 2) or 4–6 cm (Sta. 3) where ^{35}S-AVS accounted for 50, 28 and 65% of the total SRR, respectively (Fig. 1). Below this depth the role of ^{35}S-AVS declined. ^{35}S-AVS was more important at Sta. 3 than at the other stations.

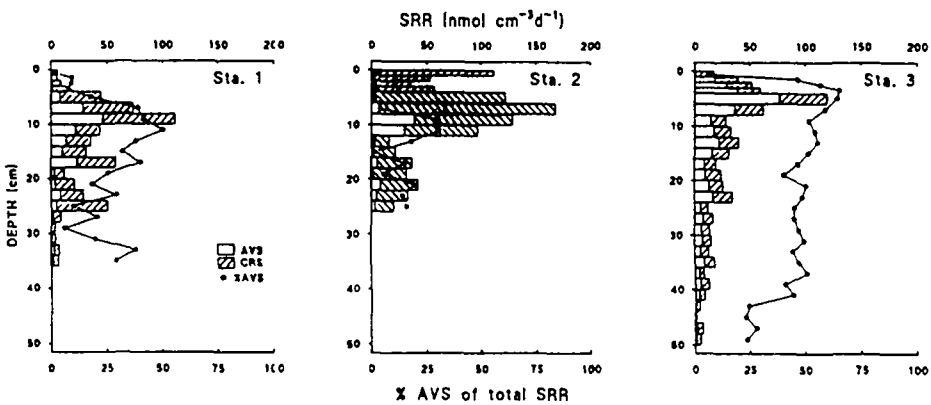

Fig. 1. Depth profiles of sulfate reduction rates at the 3 examined stations separated into the AVS and CRS fraction. Rates are based on duplicate distillations of one core and are given in nmol cm^{-3} d^{-1}. The percentage of label recovered in the AVS fraction is given as %AVS. Depth profiles of the 2 short cores are given in Kristensen et al. (1994).

The percentage of label recovered as ^{35}S–CRS (FeS_2 + S^0) predominated in the surface layers, and was > 90% at depths up to 4 cm at Sta. 1, 8 cm at Sta. 2 and 1 cm at Sta. 3.

The depth integrated sulfate reduction rates (ΣSRR) (one long core from each station) were highest at the mangrove site at Sta. 2 (Table 1). Based on the rates in the upper 10 cm (triplicate cores) ΣSRR was approximately 2 and 3 times higher at this station compared to Sta. 3 and 1 respectively. The ΣSRR_{CRS} accounted for 47% of the total ΣSRR at Sta. 3, compared to 68% and 88% at Sta. 1 and 2 respectively (Table 1).

Table 1. Integrated sulfate reduction rates (SSRR) throughout the examined sediment depth intervals (based on duplicate analysis of one core) and in the upper 0–10 cm (based on 3 cores ± SE). The percentage of the ΣSRR recovered in the CRS fraction ($\%SRR_{CRS}$) is also indicated.

	Depth cm	ΣSRR mmol m^{-2} d^{-1}	$\%SRR_{CRS}$
Sta. 1	0–38	11.21	67.5
	0–10	3.42 ± 1.41	66.1
Sta. 2	0–27	19.75 ± 2.71[a]	87.5
	0–10	10.04 ± 1.46	90.9
Sta. 3	0–53	12.87	47.2
	0–10	5.57 ± 0.40	41.4

[a] average of 2 cores.

Particulate sulfur pools. The CRS (FeS_2 + S^0) pool was the most important inorganic sulfur pool at all 3 stations (Fig. 2), being 50–100 times higher than the FeS pool (Fig. 3). There was a gradual increase in the CRS pool with depth at Sta. 1 and 2. Below 25 cm at Sta. 1, a rapid increase was evident, however, with values approaching 270 µmol g dw^{-1} at 35 cm depth. At Sta. 3 the CRS pool appeared to be lower and constant with depth at about 80 µmol g dw^{-1} (below 6 cm). The maximum pool size of FeS at Sta. 1 was found at 8–20 cm depth (2.8–4.4 µmol g dw^{-1}) coinciding with the peak in SRR_{AVS} (Fig. 1). At Sta. 3 the maximum FeS pool (Fig. 3) was found in the coral sand at 28–45 cm depth (3.6–6.9 µmol g dw^{-1}). At Sta. 2 the FeS pool was very low (< 0.4 µmol g dw^{-1}) throughout the entire depth interval examined.

The pool of particulate organic sulfur was determined analysing total particulate sulfur by CHNS analysis on sediment samples dried to 105 °C and subtracting the inorganic sulfur pools (sediment combusted at 520 °C). The inorganic sulfur (IS) pools correlated well with the CRS pools determined by distillation (stoichiometry 0.8–1.1:1 between IS and CRS; R^2 = 0.7–0.9). The organic pools increased with depth at Sta. 1 and 2 (Fig. 2). At Sta. 1, however, a slight decrease occurred in the upper 10 cm followed by a dramatic increase to a maximum of 300 µmol g dw^{-1} at 18–28 cm. At Sta. 2, maximum concentrations of 350 µmol g dw^{-1} were observed at 10 cm and 20 cm depth

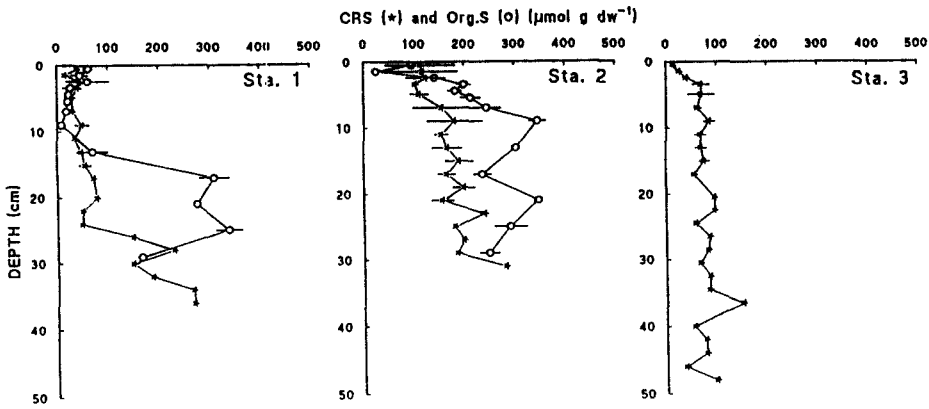

Fig. 2. Depth profiles of chromium reducible sulfur (CRS) and particulate organic sulfur (Org.S) given in µmol g dw^{-1}. CRS is the average of 3 cores (±SE), and Org.S the average of 2 cores (±SE). Org.S was not detectable at Sta. 3.

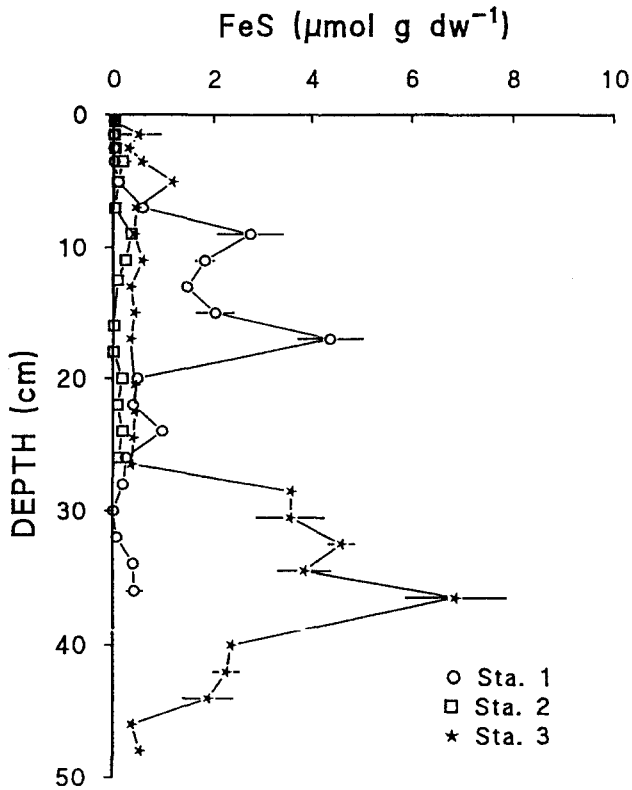

Fig. 3. Depth profiles of the FeS pool (FeS = AVS-ΣH_2S) given in µmol g dw^{-1} for the 3 stations. Values represent mean (±SE) of 2 distillations of one core.

separated by a minimum concentration of 240 μmol g dw^{-1}. For both stations organic sulfur was generally higher than the measured CRS pool (up to 2 times) except in the uppermost 5–10 cm (Fig. 2). At Sta. 3, organic sulfur was below the detection limit (< 10 μmol S g dw^{-1}) throughout the core.

Particulate iron pools. The reduced particulate iron pool, $Fe(II)_{HCl}$, extracted by 0.5 M HCl, was considerably higher (up to 4.5 μmol g dw^{-1}) than the oxidized pool, $Fe(III)_{HCl}$ (up to 1.5 μmol g dw^{-1}) at all stations (Fig. 4). The oxidized pool should, however, be considered as a minimum estimate due to oxidation artifacts during the fractionation. The largest pools were found at Sta. 1; about 5 times higher than the lowest pools which were observed at Sta. 2. $Fe(III)_{HCl}$ was highest in the uppermost 0.5 cm at all stations. Concentrations fell rapidly with depth and were depleted by 1 cm (Sta. 2), 3 cm (Sta. 3) and 6–8 cm (Sta. 1). Depth patterns of $Fe(II)_{HCl}$ showed subsurface peaks at 2 cm (4.5 μmol g dw^{-1}) and 4–8 cm (3.3 μmol g dw^{-1}) at Sta. 1 and 3, respectively (Fig. 4). The highest concentration at Sta. 2 on the other hand was observed in the uppermost cm (2.6 μmol g dw^{-1}), followed by low levels (< 1 μmol g dw^{-1}) throughout the remaining core.

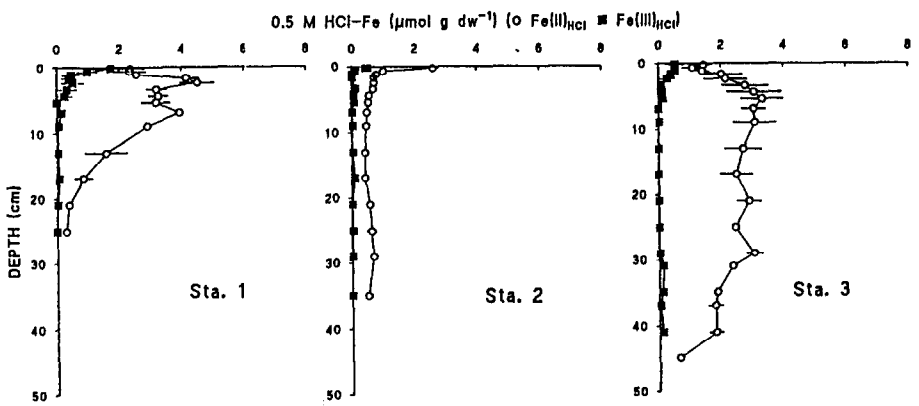

Fig. 4. Profiles of 0.5 M HCl-extractable iron separated into ferric, $Fe(III)_{HCl}$, and ferrous iron $Fe(II)_{HCl}$ given in μmol g dw^{-1}. Values are average of 2 cores (±SE).

Dissolved pools of sulfides and iron. Concentrations of dissolved sulfide (ΣH_2S) were low (0–5 μM) in the upper layers at all 3 stations (Fig. 5). At Sta. 1 no ΣH_2S (< 2 μM) was observed above 18 cm, and below this depth ΣH_2S varied irregularly from 20–250 μM. At Sta. 2, ΣH_2S appeared at 5 cm with concentrations ranging from 20 to 50 μM down to 20 cm, followed by a peak of 150 μM at 25 cm. At Sta. 3, ΣH_2S was observed below 10 cm, generally at concentrations <50 μM, with a minimum just above the coral sand, and a maximum (90 μM) within the coral sand zone.

There appeared to be a reverse correlation between ΣH_2S and dissolved

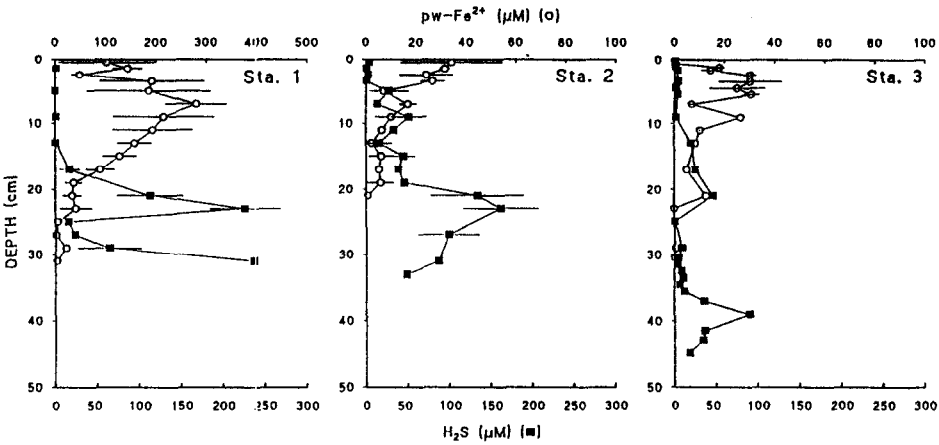

Fig. 5. Depth profiles of dissolved ferrous iron (Fe^{2+}) and dissolved sulfides (ΣH_2S) at the 3 stations. Values are given in µM and are average of 2 cores (±SE). Notice the difference in scale for ferrous iron at Sta. 1.

ferrous iron, as Fe^{2+} was found only in the upper layers where ΣH_2S was low (Fig. 5). The depth patterns of dissolved Fe^{2+} were similar to those of reduced particulate iron $Fe(II)_{HCl}$. Peak values of Fe^{2+} at all stations were found just above the layer where ΣH_2S was first detected. Maximum Fe^{2+} concentrations were higher at Sta. 1 (280 µM) than at the other stations (~35 µM).

Alkalinity, pH and sulfate. Alkalinity increased with depth at all 3 stations (Fig. 6), but values were lower than the overlying water at Sta. 1 and 2 until a depth of 12 and 5 cm, respectively. Increasing pH with depth was observed

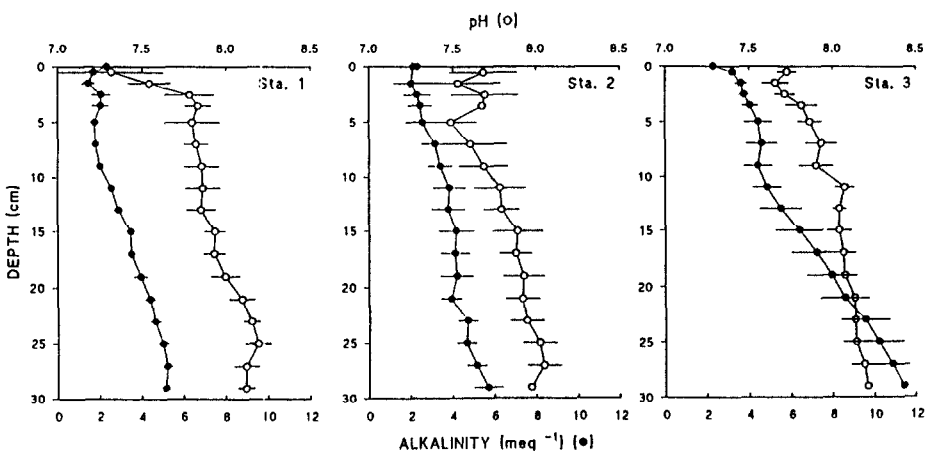

Fig. 6. Depth profiles of pH and alkalinity at the 3 examined stations. Values are given as means of 3 cores (±SE).

at Sta. 1 and 3, although values were low (7.3–7.5) in the surface layer at Sta. 1 (0–1 cm). At Sta. 2, pH was lowest at 1–2 cm depth, and values were generally lower compared to the 2 other stations throughout the examined depth interval.

Sulfate concentrations were slightly decreasing with depth at Sta. 1 from 30 to 28 mM and at Sta. 3 from 29 to 22 mM (Fig. 7). There was, however, an extraordinary high peak in the top layer at Sta. 1 (56 mM), possibly due to desiccation, as the chloride:sulfate ratio was similar to the ratio in surface waters (~20). At Sta. 2 the chloride: sulfate ratio was lower and the sulfate concentration higher in the upper 5–10 cm, indicating a surplus of sulfate in these layers (32–36 mM). Below sulfate concentrations decreased (to 28 mM) and the chloride:sulfate ratio correspondingly increased.

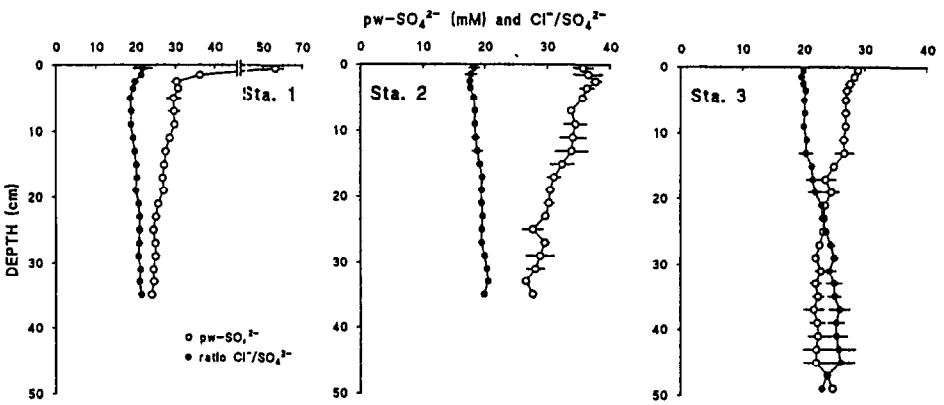

Fig 7. Depth profiles of pore water sulfate ($pw\text{-}SO_4^{2-}$) given in mM and molar chloride:sulfate ratios ($Cl^-:SO_4^{2-}$) at the 3 examined stations. Values are given as mean of 3 cores (±SE). Notice axis break at Sta. 1.

Discussion

Sulfate reduction and sulfur pools. Anaerobic metabolism measured as sulfate reduction reflected the large differences in physical and biological conditions at the 3 stations, with highest rates found in the rooted sediment (Sta. 2). Focusing only on the upper 10 cm of the sediment (Table 1), the bioturbated and physically disturbed sediments of Sta. 1 and 3 had sulfate reduction rates which are only 30–50% of those found in the rooted sediment of Sta. 2. In contrast, there were much smaller differences in the total sediment metabolism at the same stations measured as CO_2 production (31, 34 and 23 mmol m^{-2} d^{-1} at Sta. 1, 2 and 3, respectively) (Kristensen et al. 1994).

The measured SRR were within ranges previously reported for mangrove (Kristensen et al. 1992) and saltmarsh sediments (Howarth & Giblin 1983; Hines et al. 1989). Compared to an earlier study from the same area in 1990

(Kristensen et al. 1991), the present rates were surprisingly 4–7 times lower. Mangrove sediments are generally characterized by large spatial and temporal variability in both physical and biological parameters (Alongi 1989). The large temporal variation in benthic metabolism found in Ao Nam Bor between 1990 and 1992 may be explained in part by the variable quantities and qualities of the materials deposited for the two years (see detailed discussion in Kristensen et al. 1994).

During the short term SRR incubations (~12 h) a significant amount of reduced label was recovered as ^{35}S-CRS. On an areal basis the highest percentage of label recovered as ^{35}S-CRS was 88% at Sta. 2, compared with 68% at Sta. 1 and 47% at Sta. 3. In subtidal sediments an average of 20–40% of ^{35}S-label in radioassays is usually found as CRS (Howarth & Jørgensen 1984; Thode-Andersen & Jørgensen 1989; Fossing et al. 1992), but higher values have previously been measured in mangrove (Kristensen et al. 1991, 1992) and salt marsh sediments (Howarth & Giblin 1983; Howarth & Merkel 1984). A large percentage of reduced label is generally recovered as ^{35}S-CRS in oxidized surface layers of subtidal sediments (Howarth & Jørgensen 1984; Thode-Andersen & Jørgensen 1989), and the extended oxidation by burrows and roots in these mangrove sediments may be responsible for the high recovery of label as ^{35}S-CRS at Sta. 1 and 2. The ^{35}S-CRS was less important at Sta. 3, except for the surface layer, where current and wave disturbance are possible causes for oxidation and thus the high recovery. At all 3 stations the maximum amount of label as ^{35}S-AVS was found as a subsurface peak around 6–10 cm depth, as observed in subtidal (Thode-Andersen & Jørgensen 1989) and other mangrove sediments (Kristensen et al. 1992).

The most important pool of reduced inorganic sulfur was CRS at all 3 stations as is the case in most other marine sediments (Thode-Andersen & Jørgensen 1989). Pyrite is usually the primary component of the CRS pool (Thode-Andersen & Jørgensen 1989). In an earlier study of these mangrove sediments more than 99% of the CRS pool was found as pyrite (Kristensen et al. 1991), suggesting that the CRS pool measured in this study can be assumed to be pyrite. The pools of pyrite at Sta. 1 and 2 were high compared with subtidal sediments (Jørgensen et al. 1985; Kristensen et al. 1991) and salt marsh sediments (Howarth & Giblin 1983; King 1988; Oenema 1990). Pyrite was at Sta. 2 and 3 primarily formed in the upper 10 cm, whereas the concentration was increasing to a depth of 30 cm at Sta. 1 with a rapid buildup from 25 cm depth. The accumulation of FeS on the other hand, was much lower (only 1–10% of the CRS) than observed for subtidal and salt marsh sediments (Swider & Mackin 1989; Thode-Andersen & Jørgensen 1989).

Formation of iron sulfides

Extraction procedures for particulate iron vary among studies which make it difficult to compare different locations. Pools of $Fe(III)_{HCl}$ and $Fe(II)_{HCl}$ were low compared with other subtidal sediments (Higashi & Shinagawa 1985

(extracted with H_2SO_4); Oenema 1989 (extracted with NH_4-oxalate); Fossing et al. 1992 (same procedure as in this study); Wallmann et al. 1993 (1 M HCl)), but similar to other mangrove sediments (Silva et al. 1990 (0.1 M HCl, dry sediment)). The combined $Fe(II)_{HCl}$ + $Fe(III)_{HCl}$ pool was 2–3 orders of magnitude lower than the HNO_3-extractable iron pool (~400–600 μmol cm^{-3}) measured at Ao Nam Bor in 1990 (Kristensen et al. 1991).

Iron oxides are important for the oxidation of reduced sulfides, although crystalline forms of iron oxides may react slowly (Canfield 1989; Canfield et al. 1992). The inverse relationship between dissolved sulfides and Fe^{2+} in pore waters at all 3 stations (Fig. 5) suggests, that the distributions of these solutes are at least partially regulated by interaction with iron sulfide minerals. Pyrite-Fe, estimated from CRS pools was, however, much higher than the HCl-extracted iron in these layers. The low concentration of reactive iron in combination with the high sulfate reduction rates suggest iron limitation during the early diagenesis of pyrite. The accumulation of dissolved sulfides was, however, low in the surface layers, and a possible source of reactive iron oxides for pyrite formation is the large HNO_3-extractable iron pool, e.g. as crystalline forms. Pyrite-Fe accounted for 10–15% of the HNO_3-extractable pool.

At Sta. 2 the presence of roots may stimulate pyrite formation in the surface layers because: (1) active roots create oxidized microzones, which may promote the oxidation of sulfides (Thibodeau & Nickerson 1986; McKee et al. 1988), (2) roots may excrete enzymes which oxidize reduced sulfur compounds directly or indirectly by oxidizing reduced iron (Gardner 1990; Luther et al. 1991), or (3) a slightly lower pH from sulfide oxidation around the roots may stimulate pyrite formation (Rickard 1975).

Carbon and sulfur cycling. The total C:S ratio (elemental ratio between particulate organic carbon and total sulfur pool) was high (10–18) in the upper layers at Sta. 1 and 2 (Fig. 8) which is comparable to subtidal sediments (Jørgensen et al. 1990), but decreased to < 8 in the deeper parts (> 10 cm). The depth dependent decrease was primarily caused by higher concentrations of sulfur (organic as well as inorganic), as organic carbon remained almost constant with depth. This indicates a storage of sulfur in the deeper parts. The ratio was low (< 7) throughout the examined depth interval at Sta. 3 due to the low organic carbon as well as the low sulfur content compared to the 2 other stations.

The significant accumulation of organic sulfur found with depth at Sta. 1 and 2 (up to 400 μmol g^{-1} dw) has been observed previously in a mangrove peat (Altschuler et al. 1983). Organic sulfur is considered to play a minor role in the sulfur cycling in subtidal sediments, but it has been suggested as a potential storage pool in salt marsh sediments (Lord & Church 1983; Luther et al. 1986; Francois 1987; Giblin 1988; King 1988; Ferdelman et al. 1991). Several pathways for the formation of organic sulfur have been suggested, where organic sulfur most often is found in the humic fraction of sedimen-

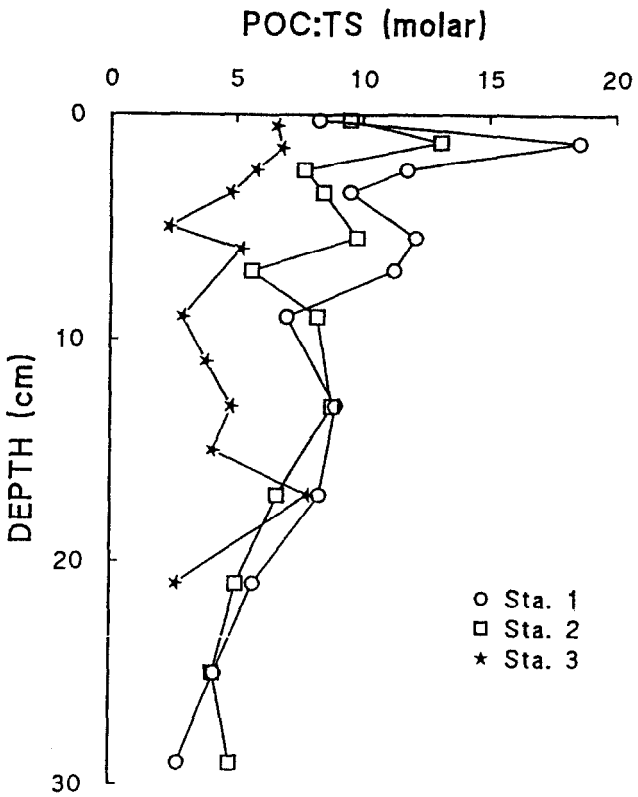

Fig. 8. Molar ratios of particulate organic carbon (POC) and total sulfur (TS) shown as a function of depth at the 3 stations.

tary organic matter derived from algal or bacterial skeletons or through sulfate reduction (Francois et al. 1987; Kohnen et al. 1990; Ferdelman et al. 1991; Urban & Brezonik 1993). During sulfate reduction under oxidized conditions sulfur enrichment of humic compounds occurs from partly oxidized sulfur compounds, whereas polysulfides may be the source under reduced conditions (Francois et al. 1987; Ferdelman et al. 1991). Organic sulfur is suggested as an important component of the sulfur cycle in sediments with high sulfate reduction rates, high dissovled sulfide concentrations and iron limitation (Ferdelman et al. 1991). At Sta. 1 and 2 the increasing concentration of organic sulfur and decreasing C:S ratio with depth indicate a formation of organic sulfur through reduced sulfur compounds and less likely due to a sedimentation of detritus as the surface concentration is low. The organic sulfur pool obtained high concentrations closer to the surface compared to the pyrite pool, and this indicate iron limitation during the formation of ironsulfides, as organic sulfur is the first sulfur compound formed. Organic sulfur is also more persistent towards reoxidation than the inorganic sulfur compounds (Ferdelman

et al. 1991). In the deeper layers pyrite is possibly formed by a slow reaction with the mineral-bound iron or crystalline iron oxides.

Reoxidation of FeS_2. Reoxidation of FeS_2 is generally caused by the same mechanisms as those driving the formation of FeS_2 in oxidized sediment layers. In the reoxidation zone, acidification and a subsequent decrease in alkalinity may develop concurrent with peaks of ferrous iron, sulfate and other oxidized sulfur compounds indicating pyrite oxidation (Lord & Church 1983; Giblin & Howarth 1984; Luther et al. 1986; Luther et al. 1991).

In the subsurface layers of Sta. 2 (1–3 cm) an increase in sulfate concentration was evident in the low pH zone indicating that reoxidation of reduced sulfides occurred. The FeS_2 pool, however, was still higher here compared to the 2 other stations, probably due to the overall high rates of sulfate reduction rates at this station. At Sta. 1 the large subsurface peak of ferrous iron corresponding with the low pH (< 7.8) and low alkalinity zone indicated that rapid reoxidation occurred in the bioturbated zone. It was not possible to detect any changes in the concentration of sulfate at this station, but other oxidized sulfur compounds were likely present. At Sta. 3, the slightly lower pH found in the surface layers was associated with a higher level of alkalinity (~3.1 meq l^{-1}) than in the overlying water. The presence of ferrous iron in the examined sediment intervals may indicate, that a continuous reoxidation of sulfides occurred throughout the sediment column. Bacterial reduction of Fe(III) may, however, also result in accumulation of Fe^{2+}, although the mechanisms behind and the importance of this process are not well known (Hines et al. 1991). Tidal currents, wave action and bioturbation may be important controlling factors involved in reoxidation of FeS_2, since this pool generally was low at this station, especially in the upper layers.

Based on measured sulfate reduction rates and the profiles of inorganic sulfur species, it is evident, that reoxidation is an important process in the sulfur cycling of mangrove sediments. Significant burial of reduced sulfur apparently occur only below the depth of bioturbation at Sta. 1, or in the deeper parts with dead roots at Sta. 2. Very little sulfur appears to be buried at Sta. 3, probably due to the extensive physical and biological disturbance at the tidal flat. Pyrite as well as organic sulfur are the important components in the storage of reduced sulfides in mangrove sediments, where organic sulfur may attain pool sizes 2 times higher than the pyrite pool. Reactive iron may be the controlling factor in pyrite formation as practically all reactive iron present in the mangrove sediments is bound as pyrite.

Acknowledgement

This work and an earlier version of this manuscript benefited from review by Gary M. King and two anonymous reviewers. We are thankful to the staff of

PMBC for providing facilities and invaluable assistance during this study. We thank Hanne Brandt for technical assistance. This work was supported by grant No. 91-0542/60 from the Carlsberg Foundation.

References

Alongi DM (1989) The role of soft-bottom benthic communities in tropical mangrove and coral reef ecosystems. Rev. Aquat. Sci. 1: 243–280

Altschuler ZS, Schnepfe MM, Silber CC & Simon FO (1983) Sulfur diagenesis in everglades peat and origin of pyrite in coal. Science 221(4607): 221–227

Andersen FØ & Kristensen E (1988) Oxygen microgradients in the rhizosphere of the mangrove *Avicennia marina*. Mar. Ecol. Prog. Ser. 44: 201–204

Canfield DE (1989) Reactive iron in marine sediments. Geochim. Cosmochim. Acta 53: 619–632

Canfield DE, Raiswell R & Bottrell S (1992) The reactivity of sedimentary iron minerals toward sulfide. Am. J. Sci. 292: 659–683

Carlson PR, Yarbro LA, Zimmermann CF & Montgomery JR (1983) Pore water chemistry of an overwash mangrove island. Florida Sci. 46(3/4): 233–238

Casagrande DJ, Siefert K, Berschinski C & Sutton N (1977) Sulfur in peat-forming systems of the Okefenokee Swamp and Florida Everglades: origins of sulfur in coal. Geochim. Cosmochim. Acta 41: 161–167

Cline JD (1969) Spectrophotometric determination of hydrogen-sulfide in natural waters. Limnol. Oceanogr. 14: 454–458

Ferdelman TG, Church TM & Luther III GW (1991) Sulfur enrichment of humic substances in a Delaware salt marsh sediment core. Geochim. Cosmochim. Acta 55: 979–988

Fossing H & Jørgensen BB (1989) Measurement of bacterial sulfate reduction in sediments: evaluation of a single-step chromium reduction method. Biogeochem. 8: 205–222

Fossing H, Thamdrup B & Jørgensen BB (1992) Havbundens svovl-, jern- og mangankredsløb i Å. Danish Environmental Protection Agency. Publication No. 15. Copenhagen

Francois R (1987) The influence of humic substances on the geochemistry of iodine in nearshore and hemipelagic marine sediments. Geochim. Cosmochim. Acta 51: 2417–2427

Gardner LR (1990) Similation of the diagenesis of carbon, sulfur, and dissolved oxygen in salt marsh sediments. Ecological Monographs 60: 91–111

Giblin A (1988) Pyrite formation in marshes during early diagenesis. Geomicrobiol. J. 6: 77–97

Giblin AE & Howarth RW (1984) Porewater evidence for a dynamic sedimentary iron cycle in salt marshes. Limnol. Oceanogr. 29(1): 47–63

Hart MGR (1959) Sulphur oxidation in tidal mangrove soils of Sierra Leone. Plant and Soil 11(3): 215–236

Higashi T & Shinagawa A (1985) Soils of a mangrove forest composed of *Rhizophora mucronata* and *Bruguiera gymnorrhiza* from Ishigaki Island, Japan. Soil Sci. Plant Nutr. 31(3): 427–435

Hines ME, Knolmeyer SL & Tugel JB (1989) Sulfate reduction and other sedimentary biogeochemistry in a northern New England salt marsh. Limnol. Oceanogr. 34(3): 578–590

Hines ME, Bazylinski DA, Tugel JB & Lyons WB (1991) Anaerobic microbial biogeochemistry in sediments from two basins in the Gulf of Maine: evidence for iron and manganese reduction. Estuar. Coast. Shelf. Sci. 32: 313–324

Howarth RW (1984) The ecological significance of sulfur in the energy dynamics of salt marsh and coastal marine sediments. Biogeochem. 1: 5–27

Howarth RW & Giblin A (1983) Sulfate reduction in the salt marshes at Sapelo Island, Georgia. Limnol. Oceanogr. 28(1): 70–82

Howarth RW, Giblin A, Gale J, Peterson BJ & Luther III GW (1983) Reduced sulfur compounds in the pore waters of a New England salt marsh. Environ. Biogeochem. Ecol. Bull. 35: 135–152

Howarth RW & Jørgensen BB (1984) Formation of ^{35}S-labelled elemental sulfur and pyrite in coastal marine sediments (Limfjorden and Kysing Fjord, Denmark) during short-term $^{35}SO_4^{2-}$ reduction measurements. Goechim. Cosmochim. Acta 48: 1807–1818

Howarth RW & Merkel S (1984) Pyrite formation and the measurement of sulfate reduction in salt marsh sediments. Limnol. Oceanogr. 29(3): 598–608

Huettel M & Gust G (1992) Impact of bioroughness on interfacial solute exchange in permeable sediments. Mar. Ecol. Prog. Ser. 89: 253–267

Jørgensen BB (1978) A comparison of methods for the quantification of bacterial sulfate reduction in coastal marine sediments. I. Measurements with radiotracer techniques. Geomicrobiol. J. 1: 11–27

Jørgensen BB (1982) Mineralization of organic matter in the sea bed – the role of sulfate reduction. Nature 296: 643–645

Jørgensen BB, Bang M & Blackburn TH (1990) Anaerobic mineralization in marine sediments from the Baltic Sea-North Sea transition. Mar. Ecol. Prog. Ser. 59: 39–54

King GM (1988) Patterns of sulfate reduction and the sulfur cycle in a South Carolina salt marsh. Limnol. Oceanogr. 33(3): 376–390

Kohnen MEL, Sinninghe Damsté JS, Kock-Van Dalen AC, Ten Haven HL, Rullkötter J & De Leeuw JW (1990) Origin and diagenetic transformations of C_{25} and C_{30} highly branched isoprenoid sulphur compounds: further evidence for the formation of organically bound sulphur during early diagenesis. Goechim. Cosmochim. Acta 54: 3053–3063

Kristensen E & Andersen FØ (1987) Determination of organic carbon in marine sediments: a comparison of two CHN-analyzer methods. J. Exp. Mar. Biol. Ecol. 109: 15–23

Kristensen E, Holmer M, Bussarawit N (1991) Benthic metabolism and sulfate reduction in a southeast Asian mangrove swamp. Mar. Ecol. Prog. Ser 73: 93–103

Kristensen E, Devol AH, Ahmed SI & Saleem M (1992) Preliminary study of benthic metabolism and sulfate reduction in a mangrove swamp of the Indus Delta, Pakistan. Mar. Ecol. Prog. Ser. 90: 287–297

Kristensen E, King GM, Holmer M, Banta GT, Jensen MH & Hansen K (1994) Sulfate reduction, acetate turnover and carbon metabolism in sediments of the Ao Nam Bor Mangrove, Phuket, Thailand. Mar. Ecol. Prog. Ser. 109(2–3): 245–255

Lord III CJ & Church TM (1983) The geochemistry of salt marshes: sedimentary ion diffusion, sulfate reduction, and pyritisation. Geochim Cosmochim. Acta 47: 1381–1391

Lovley DR & Phillips EJP (1987) Rapid assay for microbially reducible ferric iron in aquatic sediments. Appl. Environ. Microbiol. 53: 2636–2641

Luther III GW, Giblin AE & Varsolona RV (1985) Polarographic analysis of sulfur species in marine porewaters. Limnol. Oceanogr. 30(4): 727–736

Luther III GW, Church TM, Scudlark JR & Cosman M (1986) Inorganic and organic sulfur cycling in salt-marsh pore waters. Science 232: 746–749

Luther III GW, Ferdelman TG, Kostka JE, Tsamakis EJ & Church TM (1991) Temporal and spatial variability of reduced sulfur species (FeS_2, $S_2O_3^{2-}$) and porewater parameters in salt marsh sediments. Biogeochem. 14: 57–88

McKee KL, Mendelssohn IA & Hester MW (1988) Reexamination of pore water sulfide concentrations and redox potentials near the aerial roots of *Rhizophora mangle* and *Avicennia germinans*. Amer. J. Bot. 75(9): 1352–1359

Mongia AD & Ganeshamurthy AN (1989) Typical differences between the chemical characteristics of *Rhizophora* and *Avicennia* mangrove forest soils in South Andamans. Agrochimica. 33(6): 464–470

Moses CO & Herman JS (1991) Pyrite oxidation at circumneutral pH. Geochim. Cosmochim. Acta 55: 471–482

Oenema O (1990) Pyrite accumulation in salt marshes in the Eastern Scheldt, southwest Netherlands. Biogeochem. 9: 75–98

Rickard DT (1975) Kinetics and mechanism of pyrite formation at low temperatures. Am. J. Sci. 275: 636–652

Silva CAR, Lacerda LD & Rezende CE (1990) Metals reservoir in a red mangrove forest. Biotropica 22(4): 339–345

Skyring GW (1987) Sulfate reduction in coastal ecosystems. Geomicrobial. J. 5(3/4): 295–374

Stookey LL (1970) Ferrozine – a new spectrophotometric reagent for iron. Analyt. Chem. 42: 779–781

Swider KT & Mackin JE (1989) Transformation of sulfur compounds in marsh-flat sediments. Geochim. Cosmochim. Acta 53: 2311–2323

Sørensen J (1982) Reduction of ferric iron in anaerobic, marine sediment and interaction with reduction of nitrate and sulfate. Appl. Environ. Microbiol. 43: 319–324

Thibodeau FR & Nickerson NH (1986) Differential oxidation of mangrove substrate by *Avicennia germinans* and *Rhizophora mangle*. Amer. J. Bot. 73(4): 512–516

Thode-Andersen S & Jørgensen BB (1989) Sulfate reduction and the formation of ^{35}S-labeled FeS, FeS_2, and S^0 in coastal marine sediments. Limnol. Oceanogr. 34(5): 793–806

Urban NR & Brezonik PL (1993) Transformation of sulfur in sediment microcosms. Can. J. Fish. Aquat. Sci. 50: 1946–1960

Wallmann K, Hennies K, König I, Petersen W & Knauth H-D (1993) New procedure for determining reactive Fe(III) and Fe(II) minerals in sediments. Limnol. Oceanogr. 38(8): 1803–1812